 CMC, vol.38, no.1, pp.31-41, 2013

Toughening Mechanisms in Carbon Nanotube-Reinforced Amorphous Carbon Matrix Composites

J.B. Niu[1], L.L. Li[2], Q. Xu[1] and Z.H. Xia[1,3]

Abstract: Crack deflection and penetration at the interface of multi-wall carbon nanotube/amorphous carbon composites were studied via molecular dynamics simulations. In-situ strength of double-wall nanotubes bridging a matrix crack was calculated under various interfacial conditions. The structure of the nanotube reinforcement –ideal multi-wall vs. multi-wall with interwall sp^3 bonding – influences the interfacial sliding and crack penetration. When the nanotube/matrix interface is strong, matrix crack penetrates the outermost layer of nanotubes but it deflects within the nanotubes with certain sp^3 interwall bond density, resulting in inner wall pullout. With increasing the sp^3 interwall bond density, the fracture mode becomes brittle; the fracture energy decrease while the bridging strength increases and then decreases. Our results suggest that the outermost nanotube wall can serve as a sacrificial layer such that the interface may be designed by effectively putting it inside the nanotubes. Controlling the density of sp^3 interwall bond within the multiwall carbon nanotube makes the transition from brittle to tough failure modes in the composites even when the matrix/nanotube interface is strong.

Keywords: Ceramic matrix composites, modeling, interfaces, toughening.

1 Introduction

Nanocomposites with microstructures comprising of various nanofibers and nanoparticles in a lubricious matrix such as amorphous carbon (a-C) can produce superior mechanical and tribological properties. The a-C based composites with carbon nanotubes (CNT), nano-diamond, and TiC nano-particles were fabricated and reported to have high hardness, very low friction coefficient and high elastic recovery [Wilhelmsson (2007); Zehnder (2003); Pei (2005); Schittenhelm (2002); Zhou (2003);

[1] Department of Materials Science and Engineering, University of North Texas, Denton, TX 76203, USA.
[2] School of Materials Science and Engineering, Fujian University of Technology, Fuzhou 350108, China.
[3] Department of Chemistry, University of North Texas, Denton, TX 76203, USA.

Stüber (2002)]. These materials are excellent candidates for protective applications as cutting or drilling tools; however, for tribological applications, toughness or load capacity are also needed in order to prevent the brittle fracture of the coating under severe conditions.

In traditional fiber-reinforced ceramic composites, fiber/matrix interface plays an essential role in toughening. The first fracture mode in these materials is matrix cracking. If the interface is weak enough for the matrix crack to be deflected along the interface, the fibers remain intact and the composites can be tough. If the interface is too strong, the matrix crack penetrates into the fibers and the composite is brittle like a monolithic ceramic. Therefore, the crack propagation behavior at the interface is critical to toughening in fiber-reinforced ceramic composites. The mechanics of crack-interface interactions in microscale fiber composites have been addressed in several papers [He (1989); Pagano (1993); Ahn (1998); Martin (1998); Chiroiu (2010); Shen (2010); Li (2014)], which are primarily concerned with interface debonding and crack kinking. Criteria for transition from interface debonding to crack penetration were given based on energy or stress approaches. At the nanoscale, similar toughening mechanisms can occur [Xia (2004)], but the intrinsic lengths and nanostructural lengths are intertwined and so interfacial behavior may be quite different from the microscale composites. In particular, for amorphous carbon (a-C) based composite systems, both van der Waals forces and Poisson effects could be significant due to the molecular scale of the interfaces. Although some work has been done on molecular dynamics simulations of diamond and a-C composites [Li (2011); Li (2009); Namilae (2006); Kopidakis (2007); Grierson (2007)], little is known about the crack-interface interactions at the molecular scale in these materials.

The main motivation of this paper is to understand the crack deflection/penetration at the interfaces of CNT/a-C composites, i.e., brittle-to-tough transitions in the materials. Molecular dynamics simulations were performed to analyze interfacial stress and the crack deflection versus penetration for a crack with the tip on the interface in CNT/a-C composites. We show that the structure of the CNT reinforcement –ideal multi-wall vs. multi-wall with interwall sp^3 bonding – influences crack deflection/penetration. Since sp^3 bond in multi-walled CNTs can be controlled by several techniques [Peng (2008); Kis(2004)], our results thus suggest that a-C matrix composites reinforced by the multi-walled CNTs with interwall bonding can be engineered for higher toughness.

2 Models and Computational Details

We study a perpendicular matrix crack approaching the interface between a single carbon nanotube and a-C matrix in a composite. There are two possible failure

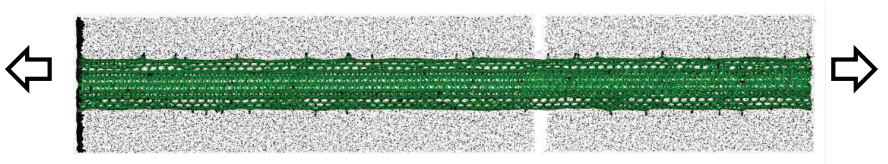

(a)

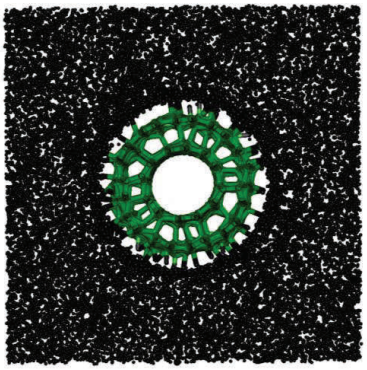

(b)

Figure 1: (a) Model of a unidirectional composite with a crack approaching the interface, and (b) top view of an atomistic model of composites with an amorphous carbon matrix and a DWCNT with inter-wall $sp^3(\rho = 0.04)$. CNTs are represented by green color and matrix is black.

paths: crack deflection on the interface; and crack penetration across the interface. Unit cells composed of a half the CNT, matrix and crack was used due to symmetry, as shown in Figure 1. Ideal double-wall CNTs (DWCNTs) in armchair configurations were generated with the graphitic C-C bond length of 0.142 nm. Nanotube diameters in the range of d = 1.66 nm with a length of $L = 20 - 40$ nm were all calculations. sp^3 bonds were introduced between DWCNT walls by a procedure described in detail in [Xia (2007)]; their density is defined as the ratio of the number of sp^3 bonds to the total number of atoms in nanotubes. The nanotube was then relaxed to equilibrium under zero applied loading. A diamond matrix of cross-sectional dimensions 3nm x 3nm was created. A hole of some diameter was then drilled out of the center of the diamond sample and a nanotube was then inserted into it. The amorphous matrix is then generated by melting at $6000 \sim 7000$K and subsequent quenching of the surrounding diamond atoms, while keeping the atoms

of the CNT frozen in their ideal positions. During the process, the matrix was allowed to expand and homogenize in a certain space such that the density of the amorphous carbon matrix can be controlled around the density of 2.0-2.3 g/cm^3. Next, the a-C matrix was cut to form a matrix crack with a width of 0.3 nm in the middle of the sample. To control the CNT/matrix interfacial strength, a layer of C atoms on the matrix surface, with a given thickness, was removed. Finally, the CNT was unfrozen and the entire system was fully relaxed to equilibrium at 0.05K.

The molecular dynamics (MD) method was used to simulate interactions between the nanotube and matrix with the software LAMMPS (Large-scale Atomic/ Molecular Massively Parallel Simulator). The interactions between atoms were calculated using an AIREBO potential [Brenner (2002)]. With a rescale thermostat to control temperature, the equations of motion were integrated with a time step of 0.8fs. The bottom and top layer of matrix and nanotube atoms is held fixed in the z-direction (pullout direction) and unconstrained in x and y. Simulation was performed by holding the two ends as a rigid body, moving along CNT axial direction at a constant speed of $\sim$2 m/s, achieving near equilibrium.

3 Results and Discussion

Multi-wall CNTs can have higher stiffness and strength than single-wall CNTs have if the external mechanical loads can be transferred to all the inner walls [Xia (2007)]. Engineering of the inter-wall coupling is possible to optimize various mechanical properties and experimental work has been done on modification of the interwall coupling in multi-wall CNTs by introducing sp^3 bonds between walls [Peng (2008); Kis (2004); Xia (2007); Byrne (2009)]. Here, we investigated the effect of interwall sp^3 bond density on the failure behaviors of free-standing DWCNTs and then crack deflection/penetration in DWCNT/a-C systems. Figure 2 shows the typical stress-strain curves of free-standing pristine and sp^3 bonded DWCNTs with a sp^3 density of 0.06. The pristine nanotube fails in brittle manner while the sp^3 bonded DWCNT is more brittle.

When CNTs are embedded into a-C matrix to form composites, sp^3 bonds can form at the a-C matrix/CNT interface. This is possible because CNTs are usually exposed to the reaction gas at elevated temperature during processing [Kothari (2012)]. Our simulation also shows that large number of sp^3 bonds are formed at CNT/a-C interface during treating process for a-C matrix, as shown in Figure 1(b). Therefore, the CNT/a-C interface is strong in CNT/a-C composites. Under such interfacial condition, bridging stress-strain curves for a CNT embedded in a-C matrix were calculated and plotted in Figure 2. For comparison, the tensile stress is defined as the bridging force divided by CNT cross-sectional area. Two typical curves were observed for this composite system. For the composites with high density of

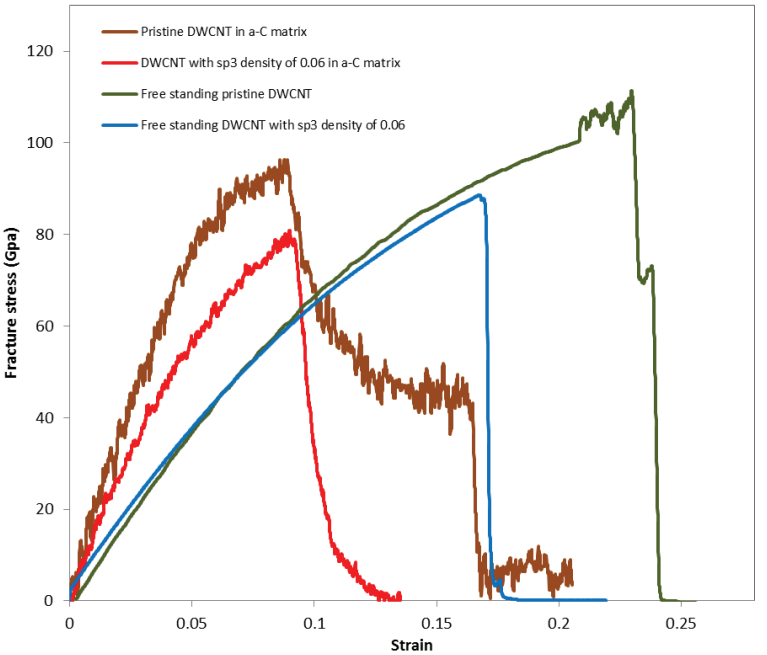

Figure 2: Stress-strain curves for free-standing DWCNTs and DWCNT/a-C composites.

sp^3 interwall bonds (ρg=0.06) in the CNTs, the bridging stress increases nearly linearly with increasing strain up to a maximum value that is defined as the bridging strength, beyond the critical stress, the further increase in strain leads to a rapid decrease of stress when two walls of DWCNTs fracture at the same time. From the stress-strain dependence, this behavior can be ascribed to the typical brittle failure mechanism. In the case of a relatively low sp^3 bond density (e.g. ρg=0.001), two peaks on stress-strain curves can be observed as shown in Figure 2, one occurs when the outermost layer fractures, and the other takes place when inner layer fails. A tail of about 10MPa can also be seen on the plot (Figure 2), which represents the pullout stress induced by the pullout of the fractured inner CNT from the outermost wall. This is a typical plastic fracture mode. In both case, no crack deflection occurs on the interface of matrix and reinforcement due to the existence of dense sp^3 bonds at the interface.

Figure 3 shows the tensile strength of DWCNTs versus the density of sp^3 bonds within the nanotubes for free-standing DWCNTs and those embedded in the a-C matrix. The tensile strength of the free-standing DWCNTs gradually reduces with

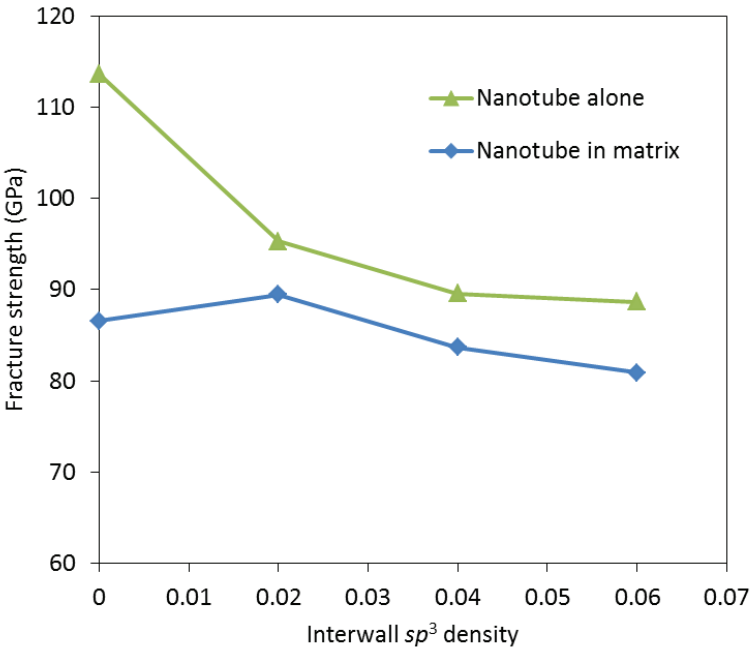

Figure 3: Fracture Strength of free-standing and bridging DWCNTs versus the density of sp^3 interwall bonds.

increasing the density of sp^3 bonds and finally levels off for sp^3 density exceeding 0.02. Most free-standing DWCNTs fail near a sp^3 bond, with failure of inner and outer walls at the same position. No pullout of inner wall from outer wall was observed in the simulations. The reduction of the strength is attributed to the sp^3 bonds, which act as defects in the nanotubes. Both the inner and outer walls are weakened by the sp^3 bonds at the same position, resulting in brittle failure of the DWCNTs. However, the effect of sp^3 interwall bonds on the strength becomes stable after sp^3 bond density exceeds 0.02.

The bridging strength of DWCNTs in a-C matrix was calculated and also plotted in Figure 3. For the pristine CNT reinforced a-C, the bridging strength reduces by over 20%. With increasing sp^3 interwall bond density, the bridging strength slightly increases and then decreases. There is an optimal sp^3 interwall bond density at which the composite strength reaches a peak. Nevertheless, all the bridging strength of CNTs embedded in the matrix is lower than that for free-standing CNTs due to the stress concentration which results in premature failure of the CNTs.

Two typical fracture modes were observed in DWCNT/a-C composites, correspond-

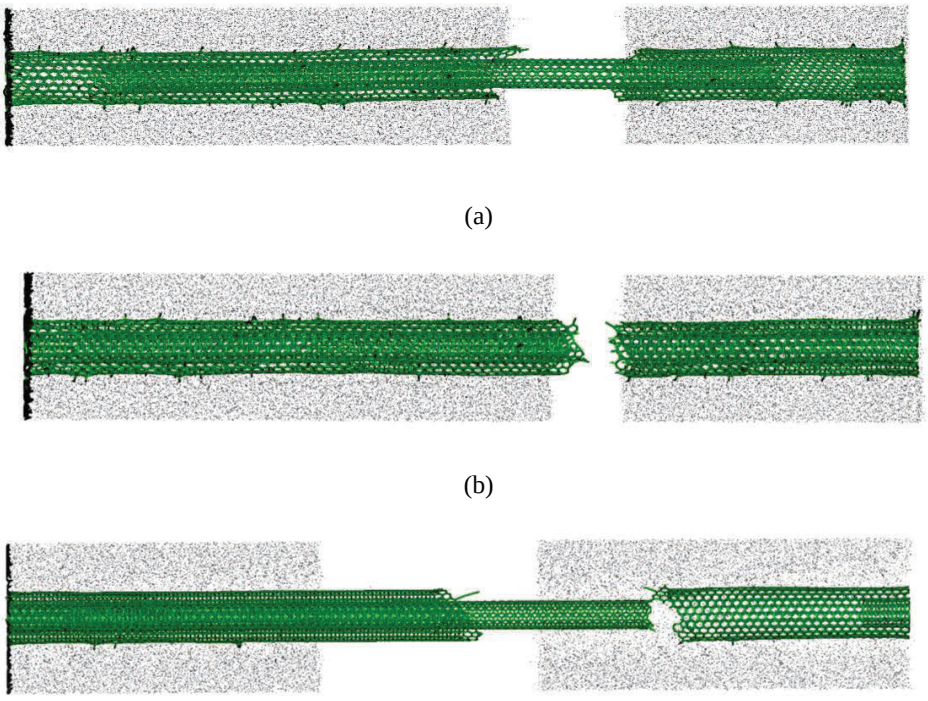

(a)

(b)

(c)

Figure 4: Failure modes of DWCNT sp^3 bonds, observed in the simulations of the nanocomposites: (a) DCNT inner wall pullout from the outer wall, (b) brittle failure, and (c) DCNT outer and inner wall pullout from matrix. Green— CNT, and black— matrix.

ing to two fracture modes described above, as shown in Figure 4. For the composites with low or no sp^3 bond within the CNTs, after the outer wall fractures at the matrix crack, the crack deflects along the interface between the outer and inner walls. As a result, the inner wall is pulled out from the outer wall (Figure 4(a)). In this mode, the outer wall works as sacrifice and protective layer during the processing and also during loading. This "sword-in-sheath" fracture mode is unique for CNT reinforced composites and has been observed experimentally in multi-wall CNT reinforced silicon nitride coatings [Kothari (2008)]. When the sp^3 bond density reaches a certain level (here $\rho > 0.02$), no crack deflection occurs between outer and inner walls of DWCNTs because of the sp^3 interwall bonds inhibit the crack propagation between CNT walls (Figure 4(b)). In addition to the fracture modes,

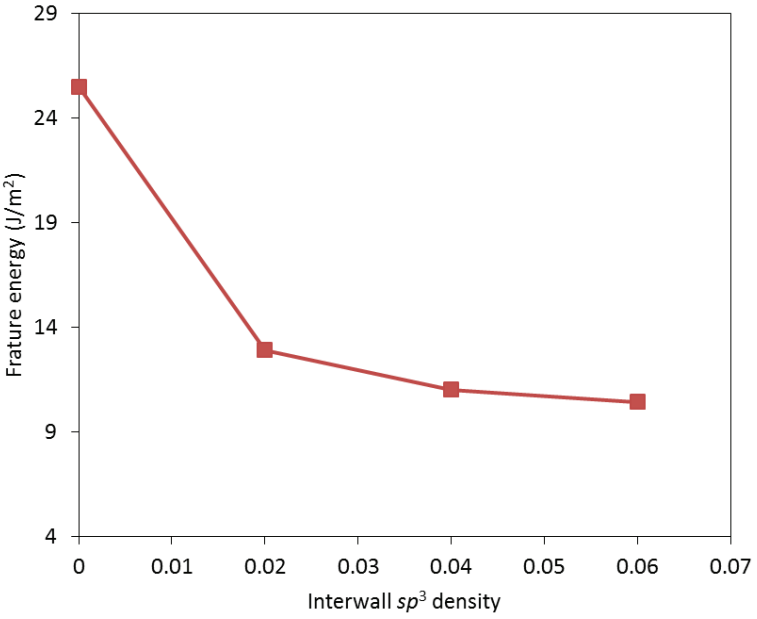

Figure 5: Fracture energy of composites versus the density of sp^3 interwall bonds.

there is the third fracture mode in which matrix crack can deflect along the matrix/fiber interface, resulting in toughening, as observed in micro-fiber reinforced composites. Here, if it lacks of sp^3 bond existing at the CNT/a-C interface, crack may deflect along the CNT/a-C interface as well, resulting in whole CNT pullout (Figure 4(c)), even for a high sp^3 interwall bond density. This type of fracture mode has also been observed in CNT reinforced alumina coatings [Xia (2004)]. Thus, for multiwall CNTs, the interfaces between the matrix and CNTs, as well as within the CNTs, can influence the fracture modes. Engineering these interfaces could increase both strength and fracture toughness of the nanocomposites.

The fracture energy was also calculated from the area under the stress-strain curves. Figure 5 shows the fracture energy for DWCNT reinforced a-C composites versus the density of inter-wall sp^3 bonds in DWCNTs. The composites with pristine CNTs show the highest fracture energy while the fracture energy of the composites rapidly decreases with increasing the sp^3 density. For example, the fracture energy for the composites with a sp^3 density of 0.04 is almost twice lower than those without sp^3 bond. Obviously, this rapid reduction in fracture energy is attributed to the density of sp^3 bonds within the CNTs, which causes the transition of failure from tough to brittle modes. From the simulation, two toughening mechanisms

were identified, namely, crack deflection and CNT pullout. Although the CNT/a-C matrix interface is strong due to the existence of dense sp^3 bonds at the CNT/a-C interface, crack deflection can still occur within the DWCNTs for low interwall sp^3 bond density. With increasing the sp^3 density in DWCNTs, possible sp^3 location will be closer to the matrix crack. Since sp^3 bonds are defects to the inner walls, stress concentration will build up around the defects during loading. The inner walls will break at the sp^3 bond close to the matrix crack, leading to short CNT pull-out, lowering the fracture energy. Overall, it is necessary to keep the sp^3 bond density at about 0.001 to achieve high strength and toughness for CNT/a-C composites.

4 Conclusions

Molecular dynamics simulations were performed to study the crack deflection/ penetration at the interfaces of DWCNT/a-C composites. The density of sp^3 bonds strongly affects the bridging strength and fracture energy. For weak interface and pristine DWCNTs, matrix crack can deflect along the interface between outermost layer and matrix as well as the interfaces between the walls within the DWCNTs. For relatively strong CNT/matrix interface matrix crack can deflect within the DWCNTs, resulting in toughening. A strong interface and relatively dense sp^3 interwall bonds leads to brittle failure of the composites. Engineering these interfaces could increase both strength and fracture toughness of the nanocomposites. Our results suggest that material design direction – the nanocomposites can be toughened by using outermost wall of CNTs as a sacrificial layer and introducing sp^3 bonds in the CNTs.

Acknowledgement: We acknowledge the support by National Science Foundation through the Contracts # CMMI-1212259 and CMMI-1266319 and Air Force Office of Scientific Research (AFOSR) MURI program (FA9550-12-1-0037).

References

Ahn, B. K.; Curtin, W. A.; Parthasarathy, T. A.; Dutton, R. E. (1998): Criteria for crack deflection/penetration criteria for fiber-reinforced ceramic matrix composites, *Compos. Sci. Technol.*, vol. 58, pp. 1775-1784.

Brenner, D. W.; Shenderova, O. A.; Harrison, J. A.; Stuart, S. J.; Ni, B.; Sinnott, S. B. (2002): A second-generation reactive empirical bond order (REBO) potential energy expression for hydrocarbons. *J. Phys.: Condens. Matter.*, vol. 14, pp. 783-802.

Byrne, E. M.; M. McCarthy, A.; Xia, Z.; Curtin, W. A. (2009): Multi-Wall Nan-

otubes can be Stronger than Single-Wall Nanotubes and Implications for Nanocomposite Design. *Phys. Rev. Lett.*, vol. 103, pp. 045502.

Chiroiu, V.; Munteanu, L.; Gliozzi, A. S. (2010): Application of Cosserat Theory to the Modelling of Reinforced Carbon Nananotube Beams. *Computers Materials and Continua*, vol. 19, no. 1, pp.1.

Grierson, D. S.; Carpick, R.W. (2007): Nanotribology of carbon-based materials. *Nano Today*, vol. 2, pp. 12-21.

He, M. Y.; Hutchinson, J. W. (1989): Crack deflection at an interface between dissimilar elastic materials. *Int J Solids Structures*, vol. 25, pp. 1053-1087.

Kis, A.; Csányi, G.; Salvetat, J-P.; Lee, T-N.; Couteau, E.; Kulik, A. J. et al. (2004): Reinforcement of single-walled carbon nanotube bundles by intertube bridging. *Nat. Mat.*, vol. 3, pp. 153-157.

Kopidakis, G.; Remediakis, I. N.; Fyta, M. G.; Kelires, P. C. (2007): Atomic and electronic structure of crystalline-amorphous carbon interfaces. *Diam. Relat. Mater.*, vol. 16, no. 10, pp. 1875-1881.

Kothari, A. K.; Hu, S.; Xia, Z.; Konca, E.; Sheldon, B. W. (2012): Enhanced fracture toughness in carbon-nanotube-reinforced amorphous silicon nitride. *Acta Mater.*, vol. 60, pp. 3333–3339.

Kothari, A. K.; Jian, K.; Rankin, J.; Sheldon. B. W. (2008): Comparison Between Carbon Nanotube and Carbon Nanofiber Reinforcements in Amorphous Silicon Nitride Coatings. *J. Am. Ceram. Soc.*, vol. 91, pp. 2743–2746.

Li, L.; Niu, J. B.; Xia, Z.; Yang, Y.; Liang, J. Y. (2011): Nanotube/matrix interfacial friction and sliding in composites with an amorphous carbon matrix. *Scripta Mater.*, vol. 65, pp. 1014-1017.

Li, L.; Niu, J. B.; Yang, Y. Q.; Xia, Z. H. (2014): Fracture and toughening mechanisms in SiC nanofiber reinforced SiC matrix nanocomposites with amorphous carbon coatings. *Computational Materials Science*, vol.83, pp.255–260.

Li, L.; Xia, Z.; Curtin, W. A.; Yang, Y. (2009): Molecular Dynamics Simulations of Interfacial Sliding in Carbon-Nanotube/Diamond Nanocomposites *J. Am. Ceram. Soc.*, vol. 92, pp. 2331-2336.

Martin, E.; Peters, P. W. M.; Leguillon, D.; Quenisset, J. M. (1998): Conditions for matrix crack deflection at an interface in ceramic matrix composites. *Mater. Sci. Eng. A*, vol. 250, pp. 291-302.

Namilae, S.; Chandra, N. (2006): Role of atomic scale interfaces in the compressive behavior of carbon nanotubes in composites. *Comp. Sci. Tech.*,vol. 66, pp. 2030-2038.

Pagano, N. J.; Brown III, H. W. (1993): The full-cell cracking mode in unidirec-

tional brittle-matrix composites. *Composites*, vol. 24, pp. 69-83.

Pei, Y. T.; Galvan, D.; Hosson, J. Th. M. De.; Cavaleiro, A. (2005): Nanostructured TiC/a-C coatings for low friction and wear resistant applications. *Surf. Coat. Technol.*, vol. 198, pp. 44-50.

Peng, B.; Locascio, M.; Zapol, P.; Li, S.Y.; Mielke, S. L.; Schatz, G. C. et al. (2008): Measurements of near-ultimate strength for multiwalled carbon nanotubes and irradiation-induced crosslinking improvements. *Nat. Nanotech.*, vol. 3, no. 10, pp. 626-631.

Schittenhelm, H.; Geohegan, D. B.; Jellison, G. E.; Puretzky, A. A.; Lance, M. J.; Britt, P. F. (2002): Synthesis and characterization of single-wall carbon nanotube–amorphous diamond thin-film composites. *Appl. Phys. Lett.*, vol. 81, pp. 2097.

Shen, H. S.; Zhu, Z. H. (2010). Buckling and postbuckling behavior of functionally graded nanotube-reinforced composite plates in thermal environments. *Computers, Materials & Continua (CMC)*, vol. 18, no. 2, pp. 155.

Stüber, M.; Leiste, H.; Ulrich, S.; Holleck, H.; Schild, D. (2002): Microstructure and properties of low friction TiC–C nanocomposite coatings deposited by magnetron sputtering. *Surf. Coat. Technol.*, vol. 150, pp. 218-226.

Wilhelmsson, O.; Råsander, M.; Carlsson, M.; Lewin, E.; Sanyal, B.; Wiklund, U.; Eriksson, O.; Jansson, U. (2007): Design of Nanocomposite Low-Friction Coatings. *Adv. Funct. Mater.*, vol. 17, pp.1611–1616.

Xia, Z. H.; Guduru, P. R.; Curtin, W. A. (2007): Enhancing Mechanical Properties of Multiwall Carbon Nanotubes via sp3 Interwall Bridging. *PRL*, vol. 98, pp. 245501.

Xia, Z.; Riester, L.; Curtin, W. A.; Li, H.; Sheldon, B. W.; Liang, J.; Chang, B.; Xu, J. M. (2004): Direct observation of toughening mechanisms in carbon nanotube ceramic matrix composites. *Acta Mater.*, vol. 52, pp. 931-944.

Zehnder, T.; Matthey, J.; Schwaller, P.; Klein, A.; Steinmann, P. -A.; Patscheider, J. (2003): Wear protective coatings consisting of TiC–SiC–a-C:H deposited by magnetron sputtering. *Surf. Coat. Technol.*, vol. 163-164, pp. 238-244.

Zhou, X. T.; Meng, X. M.; Meng, F. Y.; Li, Q.; Bello, I.; Zhang, W. J.; Lee, C. S. ; Lee, S. T.; Lifshitz, Y. (2003): Formation and structure of a-Cynanodiamond composite films by prolonged bias enhanced nucleation. *Diam. Relat. Mater.*, vol. 12, pp. 1640-164.